Available online at www.sciencedirect.com
SCIENCE DIRECT
Dyes and Pigments 71 (2006) 77–82
DYES and PIGMENTS
www.elsevier.com/locate/dyepig

Biosorption of Acid Blue 15 using fresh water macroalga *Azolla filiculoides*: Batch and column studies

T.V.N. Padmesh [a], K. Vijayaraghavan [a], G. Sekaran [b], M. Velan [a,*]

[a] *Department of Chemical Engineering, A.C. College of Technology, Anna University, Chennai 600025, India*
[b] *Department of Environmental Technology, Central Leather Research Institute, Chennai 600020, India*

Received 19 January 2005; received in revised form 11 April 2005; accepted 8 June 2005
Available online 18 August 2005

Abstract

The ability of fresh water macroalga *Azolla filiculoides* to biosorb Acid Blue 15 from aqueous solution was investigated in batch and column studies. Batch experiments were conducted to study the effect of initial solution pH and dye concentration. Langmuir and Freundlich isotherm models were used to fit the equilibrium data. The maximum dye uptake of 116.28 mg/g was observed at pH 7, according to Langmuir model. In column experiments, effects of bed height (15–25 cm), flow rate (5–15 ml/min) and initial dye concentration (50–100 mg/l) on dye removal were studied. An increase in bed height and initial dye concentration favors the dye biosorption, while the minimum flow rate produced maximum dye biosorption. At optimum bed height (25 cm), flow rate (5 ml/min) and initial dye concentration (100 mg/l), *A. filiculoides* exhibited an uptake of 35.98 mg/g of Acid blue 15. The Bed Depth Service Time model and the Thomas model were used to analyze the column experimental data and the model parameters were evaluated.

Keywords: *Azolla filiculoides*; Effluent treatment; Acid dye; Packed column; Thomas model

1. Introduction

Many industries, such as textile, paper, plastics, food, cosmetics, use dyes in order to color the products. The discharge of dye house wastewater into the environment is aesthetically displeasuring, impedes light penetration, damages the quality of the receiving streams and may be toxic to food chain organisms and to aquatic life [1].

A number of processes, like flocculation [2], chemical coagulation [2], precipitation [2], ozonation [3] and adsorption [4] have been employed for the treatment of dye bearing wastewaters. Although the above said physical and/or chemical methods have been widely used, they possess inherent limitations such as high cost, formation of hazardous byproducts and intensive energy requirements [5]. Biological processes such as biosorption [6], bioaccumulation [7,8] and biodegradation [9,10] have been proposed as potential methods for the removal of dyes from textile wastewater. Among these, biosorption is more advantageous for water treatment in that dead organisms are not affected by toxic wastes as they do not require a continuous supply of nutrients and they can be regenerated and reused for many cycles [11].

Several investigators have reported the potential of different biomaterials to biosorb dye from aqueous solutions, including bacteria [12], fungi [13] and microalgae [14]. However, the application of these materials presents few problems when operated in continuous mode; among these the solid–liquid separation is a major constrain. Even though immobilization may solve this problem, chemical costs and mechanical strength should be taken into consideration [15].

* Corresponding author. Tel.: +91 44 22203506; fax: +91 44 22352642.
E-mail address: velan@annauniv.edu (M. Velan).

0143-7208/$ - see front matter © 2005 Elsevier Ltd. All rights reserved.
doi:10.1016/j.dyepig.2005.06.003

Nomenclature

b	Langmuir model constant
C	Effluent dye concentration (mg/l)
C_0	Initial dye concentration (mg/l)
C_b	Breakthrough dye concentration (mg/l)
C_f	Final or equilibrium dye concentration (mg/l)
dc/dt	Slope of breakthrough curve from t_b to t_e (mg/l h)
F	Flow rate (ml/min)
K_a	BDST model constant (l/mg h)
k_{Th}	Thomas model constant (l/mg h)
M	Biosorbent mass (g)
m_{ad}	Dye mass adsorbed (mg)
m_{total}	Total dye mass sent to the column (mg)
N_0	Sorption capacity of bed (mg/l)
Q	Dye uptake (mg/g)
Q_0	Maximum solid-phase concentration of the solute (mg/g)
Q_{max}	Maximum dye uptake (mg/g)
t	Time (h)
t_b	Breakthrough time (h)
t_e	Exhaustion time (h)
V	Solution volume (l)
V_{eff}	Effluent volume (l)
Z	Bed height (cm)
v	Linear velocity (cm/h)

Macroalgae, on the other hand, usually possess good mechanical stability and rigidity, and have been widely used for heavy metal biosorption [16]. However, no research attention has been focused on utilization of macroalgae for dye removal. *Azolla filiculoides*, a fresh water blue green alga, has been shown to effectively bind chromium [17], zinc [18] and nickel [19] from aqueous solutions. It is commonly found in ditches, ponds, and slow moving streams and is capable of colonizing rapidly to form dense mats over water surfaces and thus imposing negative effects on the aquatic ecology [18]. Considering this, *A. filiculoides* was employed in the present study for the removal of Acid Blue 15 (AB15) in batch and column modes.

2. Materials and methods

2.1. A. filiculoides

A. filiculoides was collected from Milk producers union, Tirunelveli, India. It was then sun dried and crushed to particle sizes in the range of 1–2 mm. The crushed particles were then treated with 0.1 M HCl for 5 h followed by washing with distilled water and then kept for shaded dry. The resultant biomass was subsequently used in sorption experiments.

2.2. Batch experiments

Batch biosorption experiments were performed in a rotary shaker at 150 rpm using 250 ml Erlenmeyer flasks containing 0.2 g *Azolla* biomass in 50 ml of solution containing different AB15 concentration. After 12 h, the reaction mixture was centrifuged at 3000 rpm for 10 min. The dye content in the supernatant was determined using UV-Spectrophotometer (Hitachi, Japan) at λ_{max} 564 nm. The amount of dye biosorbed was calculated from the difference between the dye quantity added to the biomass and the dye content of the supernatant using the following equation:

$$Q = (C_0 - C_f) \times \left(\frac{V}{M}\right) \quad (1)$$

where Q is the dye uptake (mg/g); C_0 and C_f are the initial and equilibrium dye concentrations in the solution (mg/l), respectively; V is the solution volume (l); and M is the mass of biosorbent (g).

The Langmuir sorption model was chosen for the estimation of maximum AB15 biosorption by the biosorbent. The Langmuir isotherm can be expressed as:

$$Q = \frac{Q_{max} b C_f}{1 + b C_f} \quad (2)$$

where Q_{max} is the maximum dye uptake (mg/g) and b is the Langmuir equilibrium constant (l/mg). For fitting the experimental data, the Langmuir model was linearized as follows:

$$\frac{1}{Q} = \frac{1}{Q_{max}} + \frac{1}{b Q_{max} C_f} \quad (3)$$

The Freundlich model is represented by the equation:

$$Q = K C_f^{1/n} \quad (4)$$

where K and n are constants.

2.3. Column experiments

Continuous flow sorption experiments were conducted in a glass column (2 cm internal diameter and 35 cm height). At the top of the column, an adjustable plunger was attached with a 0.5 mm stainless sieve. At the bottom of the column, a 0.5 mm stainless sieve was attached followed by glass wool. A 2 cm high layer of glass beads (1.5 mm in diameter) was placed at the

column base in order to provide a uniform inlet flow of the solution into the column.

A known quantity of *A. filiculoides* was packed in the column to yield the desired bed height of the sorbent. Dye solution of known concentration at pH 7 was pumped upward through the column at a desired flow rate by a peristaltic pump (Miclins). The aliquots of dye at the outlet of the column were collected at regular time intervals.

The quantity of dye retained in the column represented by the area above the breakthrough curve (C vs. t) is obtained through numerical integration. Dividing the dye mass (m_{ad}) by the sorbent mass (M) leads to the uptake capacity (Q) of the alga [20]. Effluent volume (V_{eff}) can be calculated as follows [21]:

$$V_{eff} = Ft_e \quad (5)$$

where F is the volumetric flow rate (l/h).

Total amount of dye sent to column (m_{total}) can be calculated as follows [21]:

$$m_{total} = \frac{C_0 F t_e}{1000} \quad (6)$$

where t_e is the exhaustion time (h).

Total dye removal percent with respect to flow volume can be calculated as follows [21]:

$$\text{Total dye removal}\,(\%) = \frac{m_{ad}}{m_{total}} \times 100 \quad (7)$$

3. Results and discussion

3.1. Batch studies

Solution pH is one of the most important environmental factors, which influences both the cell surface dye binding sites and the dye chemistry in water. In batch experiments, the effect of initial solution pH on dye uptake was studied by varying the pH from 4 to 7 (Fig. 1). For each pH value, the AB15 concentration was varied from 10 to 1000 mg/l. The biosorbent dosage (4 g/l) and agitation speed (150 rpm) were kept constant. *Azolla* biomass exhibited higher uptakes at pH 7 for all concentrations examined. It was also observed that as the dye concentration increases, the uptake increases but percent removal decreases. For instance, on changing the initial AB15 concentration from 10 to 1000 mg/l, the amount biosorbed increased from 2.18 to 109.7 mg/g at pH 7. But the percent removal of AB15 decreased from 87.3 to 43.8% as the concentration is increased from 10 to 1000 mg AB15/l. This is because at lower concentration, the ratio of the initial moles of dye to the available surface area may be low and subsequently the fractional

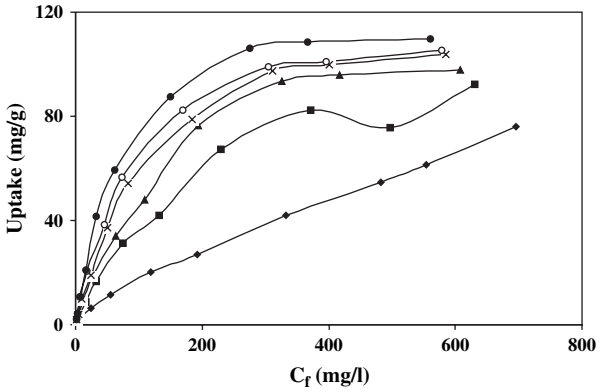

Fig. 1. Effect of pH on AB15 biosorption by *A. filiculoides* (M = 4 g/l, agitation speed = 150 rpm). (◆) pH 4; (■) pH 5; (▲) pH 5.5; (×) pH 6; (○) pH 6.5; (●) pH 7.

sorption becomes independent of initial concentration. However, at higher concentration the available sites become fewer compared to the moles of dye present and hence the percentage removal of dye is dependent upon the initial dye concentration. Also, at all pH conditions examined the isotherm curve becomes smooth and approaches the plateau value at higher dye concentrations. The plateau region of the isotherm represents well-packed dye molecules covering the entire surface area of the biosorbent [22].

The batch equilibrium data were modeled using Langmuir and Freundlich models. Table 1 shows the model constants along with correlation coefficients for biosorption of AB15 by *A. filiculoides*. Langmuir sorption model served to estimate the maximum uptake values which could not be reached in the experiments. The constant b represents affinity between biosorbent and dye. The Langmuir model parameters were largely dependent on the initial solution pH values. Both the maximum dye uptake Q_{max} and the Langmuir equilibrium constant b increase with increase in initial pH from 4 to 7. It is worth noting that both K and n values also reached their maximum values at pH 7, which implies that the binding capacity reaches the highest value and the affinity between AB15 and biomass was also higher than other pHs investigated. For all the initial pH

Table 1
Langmuir and Freundlich model parameters at different pH conditions

pH	Langmuir parameters		R^{2a}	Freundlich parameters		R^{2a}
	Q_{max} (mg/g)	b (l/mg)		K (l/g)	n	
4.0	78.13	0.0038	0.982	0.495	1.30	0.995
5.0	94.34	0.0070	0.999	1.103	1.38	0.981
5.5	99.01	0.0091	0.999	1.432	1.39	0.979
6.0	107.53	0.0098	0.999	1.687	1.41	0.969
6.5	109.89	0.0145	0.998	2.503	1.52	0.966
7.0	116.28	0.0151	0.999	2.750	1.54	0.955

[a] Correlation coefficient.

conditions (except pH 4) examined, the Langmuir model regression resulted in higher correlation coefficients than those obtained for the Freundlich model fits.

3.2. Column studies

Biosorption of AB15 by *A. filiculoides* was presented in the form of breakthrough curves (C/C_0 vs. t).

3.2.1. Effect of bed height

In the first stage of continuous experiments in column packed with *A. filiculoides*, the bed height was varied from 15 to 25 cm. In order to yield different bed heights, 6.12, 9.89 and 13.71 g of biomass were added to produce 15, 20 and 25 cm, respectively. The inlet AB15 concentration (100 mg/l) and the flow rate (5 ml/min) were kept constant. As shown in Fig. 2, both the breakthrough and exhaustion time increased with increasing bed height, which resulted in a broadened mass transfer zone. Higher uptake was observed at highest bed height due to the increase in the surface area of biosorbent, which provided more binding sites for the sorption [23,24]. Even though the breakthrough curves become steeper as the bed height decreased, a higher removal percentage was observed at the highest bed height (Table 2).

Bed Depth Service Time (BDST) is a simple model, which states that bed height (Z) and service time (t) of a column bears a linear relationship. The equation can be expressed as [25]:

$$t=\frac{N_0 Z}{C_0 v}-\frac{1}{K_a C_0}\ln\left(\frac{C_0}{C_b}-1\right) \tag{8}$$

where C_b is the breakthrough dye concentration (mg/l); N_0 is the sorption capacity of bed (mg/l); v is the linear velocity (cm/h); and K_a is the rate constant (l/mg h). This simplified design model ignores the intraparticle mass transfer resistance and external film resistance such that the adsorbate is adsorbed onto the adsorbent surface directly. With these assumptions the BDST model works well and provides useful modeling equations for the changes in system parameters [26]. The column service time was selected as the time when the effluent dye concentration reached 1 mg/l. The plot of service time against bed height at a flow rate of 5 ml/min (graph not presented) was linear ($R^2 = 0.9778$) indicating the validity of BDST model for the present system. The sorption capacity of the bed per unit bed volume, N_0, was calculated from the slope of BDST plot, assuming initial concentration, C_0, and linear velocity, v, as constant during the column operation. The rate constant, K_a, calculated from the intercept of BDST plot, characterizes the rate of solute transfer from the fluid phase to the solid phase [27]. The computed N_0 and K_a were 4395 mg/l and 0.009 l/mg h, respectively. The BDST model parameters can be useful to scale up the process for other flow rates without further experimental run.

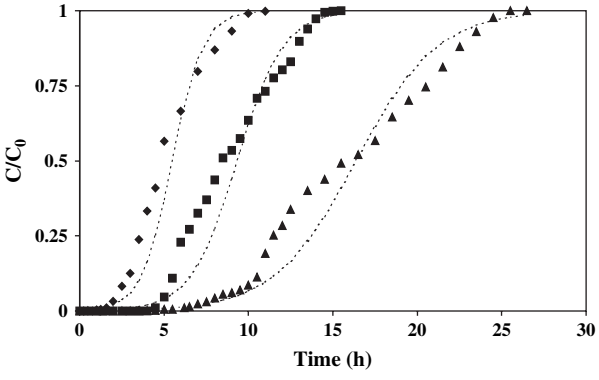

Fig. 2. Breakthrough curves for AB15 biosorption onto *A. filiculoides* biomass at different bed heights (flow rate = 5 ml/min, initial AB15 concentration = 100 mg/l, pH = 7.0). Bed heights: (◆) 15 cm; (■) 20 cm, (▲) 25 cm; (- - -) predicted from Thomas model.

3.2.2. Effect of flow rate

The influence of flow rate on biosorption of AB15 by *A. filiculoides* was investigated by keeping initial dye concentration (100 mg/l) and bed height (25 cm) constant and varying the flow rate from 5 to 15 ml/min (Fig. 3). In contrast to bed height results, the column performed well at lowest flow rate. Earlier breakthrough time appeared for highest flow rate, resulting in low uptake and least percent removal. This behavior may be due to insufficient time for the solute inside the column and the diffusion limitations of the solute into the pores of the sorbent at higher flow rates [26].

3.2.3. Effect of initial dye concentration

The biosorption performance of *A. filiculoides* on AB15 was examined at different inlet dye concentration. The breakthrough curves obtained by changing AB15 concentration from 50 to 100 mg/l at 5 ml/min flow rate and 25 cm bed height are shown in Fig. 4. A decreased inlet AB15 concentration gave an extended breakthrough curves and the treated volume was also higher, since the lower concentration gradient caused a slower transport due to decreased diffusion coefficient [21]. At the highest AB15 concentration (100 mg/l) the *Azolla* bed was saturated quickly leading to earlier breakthrough and exhaustion time. From Table 2, it was observed that the highest uptake and high percent removal of AB15 were obtained for highest AB15 concentration. Also more favorable and steep breakthrough curve was obtained for 100 mg AB15/l. The driving force for biosorption is the concentration difference between the dye on the biosorbent and the dye in the solution [21]. Thus high driving force due to high AB15 concentration resulted in better column performance.

Table 2
Column data and parameters obtained at different bed heights, flow rates and initial dye concentrations

Bed height (cm)	Flow rate (ml/min)	Initial dye concentration (mg/l)	t_b (h)	t_e (h)	Uptake (mg/g)	dc/dt (mg/l h)	V_{eff} (l)	Dye removal (%)
15	5	100	1.6	11.0	25.92	11.90	3.30	48.06
20	5	100	4.5	15.5	28.85	9.41	4.65	61.04
25	5	100	6.2	26.5	35.98	5.52	7.95	61.26
25	10	100	1.2	14.0	30.55	7.16	8.40	49.85
25	15	100	0.2	11.0	29.78	9.88	9.90	41.25
25	5	75	9.3	34.7	34.74	3.30	10.41	61.01
25	5	50	13.2	50.8	32.95	1.50	15.24	59.29

3.2.4. Application of the Thomas model

Successful design of a column sorption process required prediction of the concentration–time profile or breakthrough curve for the effluent [28]. Various mathematical models can be used to describe fixed bed adsorption. Among these the Thomas model is simple and widely used by several investigators [21,28]. The column biosorption data obtained at different bed heights, flow rates and dye concentrations were fitted using Thomas model. The linearized form of Thomas model can be expressed as follows [28]:

$$\ln\left(\frac{C_0}{C}-1\right)=\frac{k_{Th}Q_0M}{F}-\frac{k_{Th}C_0}{F}V \quad (9)$$

where k_{Th} is the Thomas model constant (l/mg h), Q_0 is the maximum solid phase concentration of solute (mg/g), and V is the throughput volume (l). The model constants k_{Th} and Q_0 can be determined from the plot of $\ln[(C_0/C)-1]$ against t [21]. Comparison of experimentally determined and Thomas model predicted breakthrough curves is shown in Figs. 2–4. In general, good fits were obtained in all cases with correlation coefficients ranging from 0.983 to 0.994. Table 3 summarizes the Thomas model parameters obtained at different bed heights, flow rates and initial AB15 concentrations. As bed height increased, the values of Q_0 increased and the values of k_{Th} decreased. The bed capacity Q_0 decreased and Thomas constant k_{Th} increased with increasing flow rate. Similarly, Aksu and Gönen (2004) observed that as the flow rate increased, the bed capacity decreased and Thomas constant increased for phenol biosorption to Mowital® B30H resin immobilized activated sludge. In contrast, Q_0 increased and k_{Th} decreased with increasing initial AB15 concentration. Also, in most cases a negligible difference between the experimental and predicted values of the bed capacity was observed although the deviations of experimental data from predicated values were most pronounced at higher flow rates.

4. Conclusions

This study showed that the fresh water alga *A. filiculoides* was effective in the removal of AB15. Batch experiments provided fundamental information regarding optimum pH and maximum dye uptake. Column experiments were performed in a packed column, as it makes the best use of the concentration difference known to be a driving force for adsorption. A series of column studies revealed that bed height, flow rate and initial dye concentration affected dye biosorption. The highest bed height (25 cm), lowest flow rate

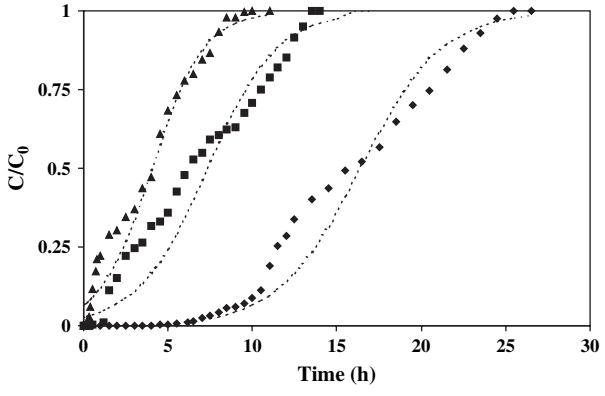

Fig. 3. Breakthrough curves for AB15 biosorption onto *A. filiculoides* biomass at different flow rates (bed height = 25 cm, initial AB15 concentration = 100 mg/l, pH = 7.0). Flow rates: (◆) 5 ml/min, (■) 10 ml/min, (▲) 15 ml/min; (- - -) predicted from Thomas model.

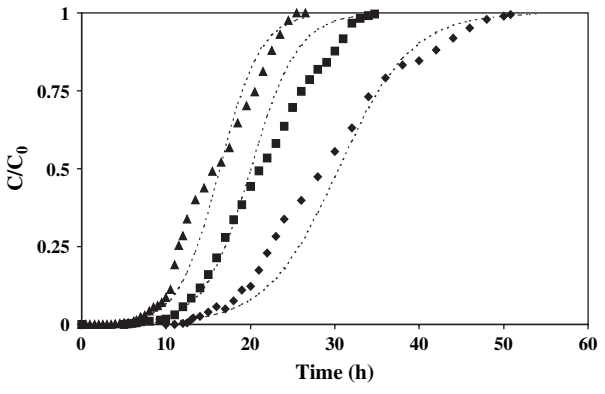

Fig. 4. Breakthrough curves for AB15 biosorption onto *A. filiculoides* biomass at different dye concentrations (bed height = 25 cm, flow rate = 5 ml/min, pH = 7.0). Initial dye concentrations: (◆) 50 mg/l, (■) 75 mg/l, (▲) 100 mg/l; (- - -) predicted from Thomas model.

Table 3
Thomas model parameters at different conditions

Bed height (cm)	Flow rate (ml/min)	Initial dye concentration (mg/l)	Q_0 (mg/g)	k_{Th} (l/mg h)	R^{2a}
15	5	100	26.88	0.0111	0.985
20	5	100	28.31	0.0073	0.987
25	5	100	35.82	0.0042	0.987
25	10	100	32.03	0.0049	0.983
25	15	100	26.48	0.0065	0.994
25	5	75	35.50	0.0044	0.992
25	5	50	33.33	0.0047	0.993

[a] Correlation coefficient.

(5 ml/min) and highest dye concentration (100 mg/l) performed well in AB15 biosorption.

A successful biosorption process not only depends on dye uptake performance of the biomass, but also on the constant supply of the biomass for the process. Therefore it is preferable to use biomass, which is either an industrial waste or available plenty in nature. *A. filiculoides* is one of the most abundantly available and rapidly reproducing fresh water algae. Also the cultivation method of *A. filiculoides* is simple and also incurs low production cost. Thus, *A. filiculoides* possesses all intrinsic characteristics to be employed for the treatment of Acid Blue 15 bearing industrial effluents.

References

[1] Talarposhti AM, Donnelly T, Anderson GK. Color removal from a simulated dye wastewater using a two-phase anaerobic packed bed reactor. Water Res 2001;35(2):425–32.

[2] Vanderviere PC, Bianchi R, Verstraete W. Treatment and reuse of wastewater from the textile wet processing industry: review of emerging technologies. J Chem Technol Biotechnol 1998;72: 289–302.

[3] Strickland AF, Perkins WS. Decolorization of continuous dyeing wastewater by ozonation. Text Chem Color 1995;27(5):11–5.

[4] Ho YS, McKay G. Sorption of dye from aqueous solution by peat. Chem Eng J 1998;72(2):115–24.

[5] Venkata Mohan S, Vijay Bhaskar Y, Karthikeyan J. Biological decolorization of simulated azo dye in aqueous phase by algae *Spirogyra* species. Int J Environ Pollut 2003;21(3):211–22.

[6] Ramakrishna KR, Viraraghavan T. Dye removal using low cost adsorbents. Water Sci Technol 1997;36(2–3):189–96.

[7] Gupta GS, Shukla SP, Parasad G, Singh VN. China clay as an adsorbent for dye house wastewater. Environ Technol 1992;13: 925–36.

[8] Aksu Z. Reactive dye bioaccumulation by *Saccharomyces cerevisiae*. Process Biochem 2003;38(10):1437–44.

[9] Chao WL, Lee SL. Decolorization of azo dyes by three white rot fungi: influence of carbon source. World J Microbiol Biotechnol 1994;10:556–9.

[10] Banat IM, Nigam P, Singh D, Marchant R. Microbial decolorization of textile-dye-containing effluents: a review. Bioresour Technol 1996;58:217–27.

[11] Vieira RHSF, Volesky B. Biosorption: a solution to pollution? Int Microbiol 2000;3:17–24.

[12] Chang JS, Chou C, Lin YC, Lin PJ, Ho JY, Hu TL. Kinetic characteristics of bacterial azo dye decolorization by *Pseudomonas luteola*. Water Res 2001;35(12):2841–50.

[13] Fu Y, Viraraghavan T. Removal of a dye from an aqueous solution by fungus *Aspergillus niger*. Water Qual Res J Canada 2000;35(1):95–111.

[14] Wafaa MA, Hassan M, Khalafallah M. Microflora involved in textile dye waste removal. J Basic Microbiol 2003;43(3):167–74.

[15] Veglio F, Beolchini F. Removal of metals by biosorption: a review. Hydrometallurgy 1997;44:301–16.

[16] Volesky B, Holan ZR. Biosorption of heavy metals. Biotechnol Prog 1995;11:235–50.

[17] Zhao M, Duncan JR. Batch removal of hexavalent chromium by *Azolla filiculoides*. Appl Biochem Biotechnol 1997;26:179–83.

[18] Zhao M, Duncan JR, Van Hille RP. Removal and recovery of zinc from solution and electroplating effluent using *Azolla filiculoides*. Water Res 1999;33(6):1516–22.

[19] Zhao M, Duncan JR. Removal and recovery of nickel from aqueous solution and electroplating rinse effluent using *Azolla filiculoides*. Process Biochem 1998;33:249–55.

[20] Volesky B, Weber J, Park JM. Continuous-flow metal biosorption in a regenerable *Sargassum* column. Water Res 2003;37:297–306.

[21] Aksu Z, Gönen F. Biosorption of phenol by immobilized activated sludge in a continuous packed bed: prediction of breakthrough curves. Process Biochem 2004;39:599–613.

[22] Sankar M, Sekaran G, Sadulla S, Ramasami T. Removal of diazo and triphenylmethane dyes from aqueous solutions through an adsorption process. J Chem Technol Biotechnol 1999;74:337–44.

[23] Zulfadhly Z, Mashitah MD, Bhatia S. Heavy metals removal in fixed-bed column by the macro fungus *Pycnoporus sanguineus*. Environ Pollut 2001;112:463–70.

[24] Vijayaraghavan K, Jegan J, Palanivelu K, Velan M. Removal of nickel(II) ions from aqueous solution using crab shell particles in a packed bed up-flow column. J Hazard Mater 2004;113B(1–3): 223–30.

[25] Hutchins RA. New method simplifies design of activated carbon systems. Chem Eng 1973;80:133–8.

[26] Ko DCK, Porter JF, McKay G. Optimised correlations for the fixed-bed adsorption of metal ions on bone char. Chem Eng Sci 2000;55:5819–29.

[27] Cooney DO. Adsorption design for wastewater treatment. Boca Raton: CRC press; 1999.

[28] Yan G, Viraraghavan T. Heavy metal removal in a biosorption column by immobilized *M. rouxii* biomass. Bioresour Technol 2001;78:243–9.